The Structures and Thermodynamics of Complexes between Water-Soluble Calix[4]arenes and Dipyridinium Ions

Yu Liu,*[a] Dong-Sheng Guo,[a] En-Cui Yang,[a] Heng-Yi Zhang,[a] and Yan-Li Zhao[a]

Keywords: Calixarenes / Conformation analysis / Inclusion compounds / Nitrogen heterocycles / Thermodynamics

Three crystalline complexes were prepared by the inclusion complexation of *p*-sulfonatothiacalix[4]arene (TCAS) and *p*-sulfonatocalix[4]arene (CAS) with 2,2′-dipyridinium (2-DPD; (complexes **1** and **2**, respectively), and TCAS with 4,4′-dipyridinium (4-DPD; complex **3**). The crystal structures show that the calixarenes in **1** and **2** maintain their original cone conformation, with shallow inclusion of 2-DPD, and assemble themselves into bi-layer arrangements. However, the cone shape of TCAS in **3** is disrupted by 4-DPD to assume the so-called 1,2-alternate conformation in the solid state, which is similar to the 1,3-alternate case of CAS stabilized by 4-DPD (**4**). The thermodynamics of this inclusion complexation were further investigated by microcalorimetric titration in aqueous solution. The obtained results indicated that the molecular binding ability and selectivity of TCAS/CAS with DPDs is entirely controlled by enthalpy gains accompanied by a smaller negative entropic change; these are discussed from the viewpoint of electrostatic, hydrogen-bonding, π-stacking, and van der Waals interactions, size/shape-fit, and a desolvation effect between host and guest. The molecular selectivity for the inclusion complexation of 2-DPD with CAS was found to be nine times greater than that of 4-DPD with CAS. Combining the present crystal structures and thermodynamic parameters revealed that the position of the nitrogen atoms in the DPDs is the crucial factor for controlling the binding modes, molecular selectivity, conformational features, and assembly behavior of the host upon complexation with TCAS/CAS. This will help us to design large molecular assemblies possessing highly supramolecular architectures based on calixarenes by controlling exactly the guest molecules.

Introduction

Calixarenes are a class of macrocycles that are generally made up of phenol units linked by methylene bridges.[1] During the last two decades, the molecular recognition and assembly of calixarenes has attracted a lot of attention because of their potential applications in various fields such as analysis and separation,[2,3] materials science,[4] enzyme-mimetic systems,[5] self-assembling membranes,[6] etc. In order to explore further the functions of calixarenes in aqueous solution, water soluble *p*-sulfonatocalix[*n*]arenes have been synthesized.[7] As they possess a π-electron-rich cavity and strongly hydrophilic upper and lower rims, with a hydrophobic cavity and outer midsection, *p*-sulfonatocalix[*n*]arenes are becoming increasingly important in the fields of supramolecular chemistry and crystal engineering, and show interesting inclusion properties and a wide range of metal coordination complexes both in solution and in the solid state.[8] Among them, *p*-sulfonatocalix[4]arene (CAS) is the most popular supramolecular building block as it forms various kinds of supramolecular aggregations[9] including bilayers,[10] capsules,[11] spheres and tubular arrays,[12] and water-filled channels,[13] etc.

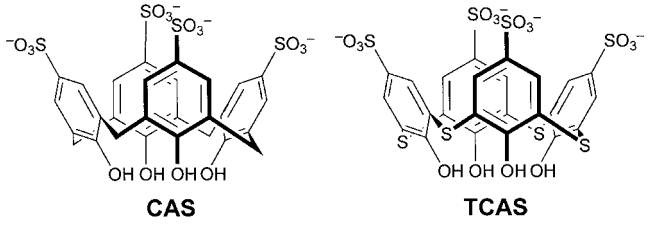

Thiacalixarenes[14,15] are a new family of calixarenes where all of the methylene linkages have been replaced by sulfur. They possess an enlarged hydrophobic cavity, have a greater degree of flexibility of the framework, are less electron-rich, and have additional binding sites. A water soluble derivative, thiacalix[4]arene tetrasulfonate (TCAS),[16] has many unique inclusion complexation properties with several neutral and charged inorganic and organic species in solution.[17−25] In the crystalline state, TCAS does not only bond guest molecules to form inclusion complexes with different conformations, such as common cone,[26] 1,2-alternate,[18] or partial-cone,[27] but can also construct supramolecular aggregations possessing bilayer or aqua-channel[27] structures. These investigations also revealed that the guest molecules exert an extraordinary influence over the binding

[a] Department of Chemistry, State Key Laboratory of Elemento-Organic Chemistry, Nankai University,
Tianjin 300071, P. R. China
Fax: (internat.) + 86-22-2350-3625
E-mail: yuliu@public.tpt.tj.cn

  DOI: 10.1002/ejoc.200400620

modes, conformational features, and assembly behavior upon complexation of both CAS and TCAS. However, to the best of our knowledge, there are few studies focused on understanding how the slight difference between host or guest structures affects the inclusion modes and binding abilities of the resulting calixarene complexes both in solution and the solid state,[28] although such studies are very significant for comprehension of the correlation between the structural feature and the molecular-recognition ability of the host-guest complexes.

In the present work we wish to report three crystal structures — the inclusion complexation of TCAS with 2,2′-dipyridinium (2-DPD) (**1**), CAS with 2-DPD (**2**), and TCAS with 4,4′-dipyridinium (4-DPD) (**3**) — and the thermodynamic origins of the molecular selectivity of binding between TCAS/CAS and DPDs in aqueous solution. It is of particular interest to examine the influence of the different heteroatom position in DPDs on the conformational features, binding ability, and assembly behavior of CAS or TCAS. A comparison of the crystal structures with the thermodynamic parameters of the resulting complexes of CAS/TCAS and DPDs, together with the reported complex of CAS with 4-DPD (**4**),[29] will help us to understand the mechanism of molecular recognition and assembly of the calixarenes.

Results and Discussion

Crystal Structures

Complexes **1**−**3** crystallize in the triclinic space group $P\bar{1}$, the monoclinic space group $P2_1/n$, and the triclinic space group $P\bar{1}$, respectively, with the asymmetric unit comprising one TCAS, 2.5 2-DPD, and 4.5 water molecules of crystallization for **1**, one CAS (two of its sulfonate groups are protonated), one diprotonated 2-DPD, and 7.5 water molecules of crystallization for **2**, and one TCAS, 2 4-DPDs, and two water molecules of crystallization for **3**. Among these crystal structures, the calixarenes in **1** and **2** retain the cone conformation, with 2-DPD included in the cavity, and present extended structures of bilayer arrangements, with each layer being composed of π-stacked calixarenes in opposite directions. However, the common cone-shape of TCAS in **3** is disrupted by 4-DPD, which forms complicated intermolecular hydrogen-bonding interactions and enforces a novel 1,2-alternate conformation. In light of the 1,3-alternate conformer of CAS stabilized by 4,4′-DPD,[29] one may reasonably deduce that the difference of the heteroatom position in DPD plays a critical role in influencing the conformational features and even assembly behavior of the host molecules, which is in agreement with our previous results.[30]

In the structure of **1** there are 2.5 2-DPD cations per unit cell and one TCAS anion; the two *cis*-2-DPDs are monoprotonated and the other half *trans*-2-DPD and one of the sulfonate groups of the calixarene are also protonated. As shown in Figure 1, one of the pyridine rings in 2-DPD penetrates into the cavity of TCAS to a depth of 4.388 Å[31] and is stabilized by the formation of one nonconventional hydrogen bond (C31−O16: 3.115 Å). The angle made by the plane of the aromatic guest with the plane of the S atoms is 63.0°. The other 2-DPD counterions are restricted in the hydrophilic or hydrophobic layer. In addition, a dimeric arrangement is observed in which the 2-DPD included within the thiacalixarene cavity is linked to a sulfonate group of the thiacalixarene in an adjacent layer by an N−H···O hydrogen-bonding interaction (N2−O14: 2.806 Å) across the hydrophilic layer (Figure 2). In this case, the

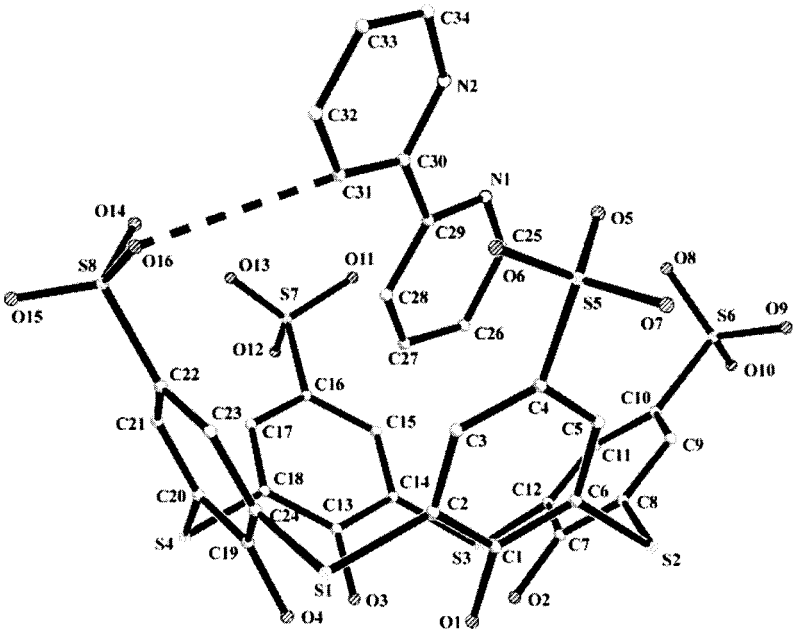

Figure 1. View of the crystal structure of **1**; the other 2-DPDs, disordered water molecules, and all the hydrogen atoms have been omitted for clarity; the broken line between O16 and C31 represents the host-guest nonconventional hydrogen bonds

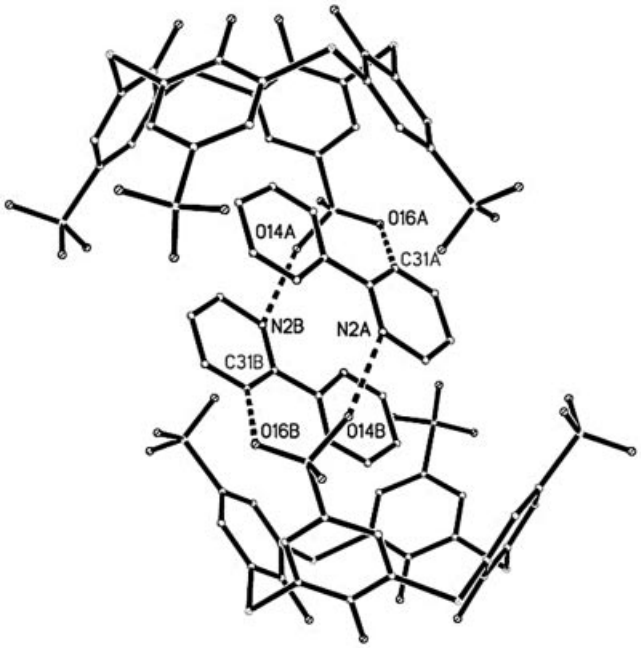

Figure 2. A *head-to-head* dimer called as slipped capsule in the crystal structure of **1**; it is formed by the conjunction of hydrogen bonds between host and guest; the other 2-DPDs, disordered water molecules, and all the hydrogen atoms have been omitted for clarity

thiacalixarene unit adopts a conventional cone configuration of approximate C_{4v} symmetry with all the oxygen atoms of the phenolic hydroxy groups in a nearly coplanar arrangement. The four aromatic rings constituting the wall of the calix are nearly upright, with corresponding dihedral angles of 63.9°, 66.7°, and 79.1°, respectively. The S···S (trans sulfonate) approaches are nearly equidistant (S5−S7: 10.726 Å; S6−S8: 11.152 Å). Furthermore, the *head-to-head* dimer further self-assembles in the common up-down fashion to form clay-like bilayer supramolecules with the hydrophobic midsections of adjacent molecules mutually aligned through intermolecular π-stacking interactions, with ring-centroid separations of 3.637 Å (C7−C12 ring···C7−C12 ring) and 3.847 Å (C13−C18 ring···C13−C18 ring); it is also stabilized by a hydrogen bond (O3−O12: 2.455 Å; Figure 3).

In the structure of **2**, 2-DPD is included into the cavity of CAS to a depth of 4.381 Å, with an angle between the plane of the aromatic guest and the plane of the methylene bridges of 48.9°. There are two clear edge-to-face π-stacking interactions between the included 2-DPD portion and the aromatic rings of CAS to reinforce the host-guest complexation. The C30−H30 bond of the 2-DPD points towards the center of the C16−C21 ring with an H30···ring centroid distance of 2.575 Å and an C30−H30···centroid angle of 160.6°. The C29−H29 bond points towards the center of the C23−C28 ring with an H29···ring centroid distance of 2.724 Å and a C29−H29···centroid angle of 162.8°. Accordingly, the cavity of CAS is forced apart somewhat to C_{2v} symmetry, with S···S approaches of 9.932 Å (S1−S3) and 11.181 Å (S2−S4), although the calixarene framework retains its cone shape in which the four aromatic

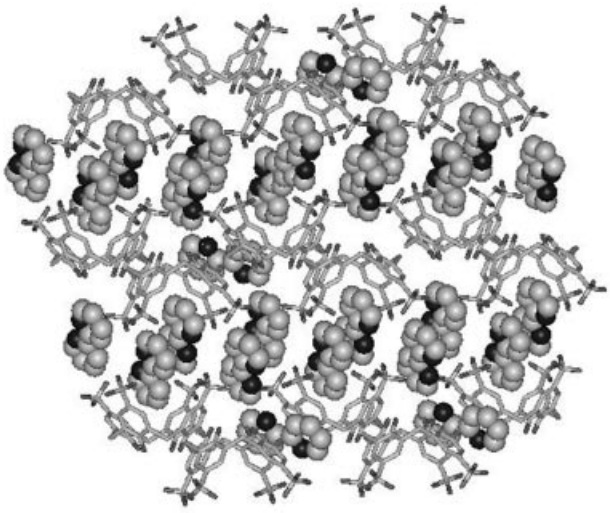

Figure 3. Bilayer packing in the crystal structure of **1** through π···π interactions; only 2-DPD molecules are space-filled; disordered water molecules and hydrogen atoms have been omitted for clarity

rings constituting the wall of the calix form angles of 68.8°, 62.0°, and 67.6°, respectively (Figure 4). The conformational distortion of CAS in **2** is reasonable because the cleft-shaped C_{2v} conformation of CAS is particularly suited to the inclusion of planar, aromatic guest species.[13] The packing structure of **2** is shown in Figure 5 and show that CAS arranges itself into a conventional bilayer arrangement by an interplay between the C−H groups and the aromatic ring involving the methylene groups of the calixarenes[32] (C15−H···centroid of C2−C7 ring: 3.375 Å; C22−H···centroid of C9−C14 ring: 3.687 Å; C8−H···centroid of C23−C28 ring: 3.312 Å; C1−H···centroid of C16−C21 ring: 3.365 Å;). In addition, the closest O3···O5 contact is 3.070 Å, which indicates that

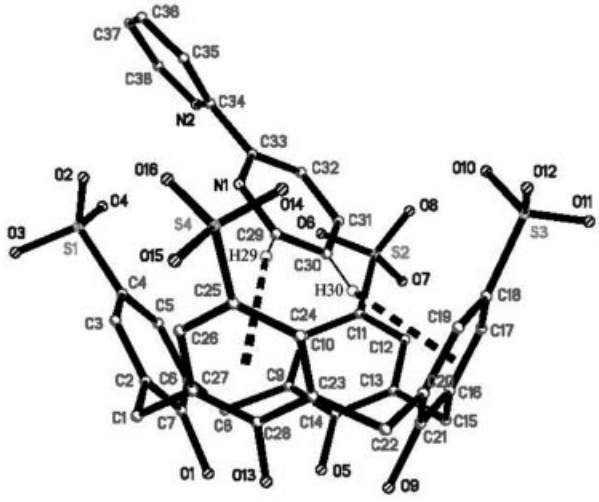

Figure 4. View of complex **2**; water molecules, counterions, and hydrogen atoms have been omitted for clarity

weak hydrogen bonding likely helps to stabilize the bilayer arrangements.

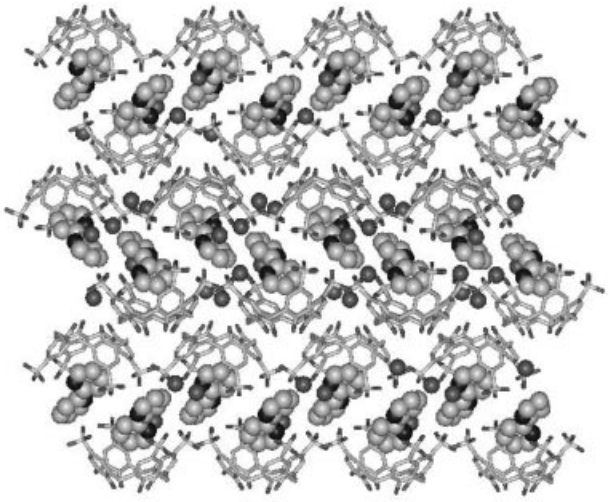

Figure 5. B-layer packing in the crystal structure of **2** through C-H···π interactions; only 2-DPD molecules are space-filled; disordered water molecules and hydrogen atoms have been omitted for clarity

In general, CAS or TCAS organize themselves in an up-down fashion to form a clay-like bilayer with the hydrophobic midsections of adjacent molecules mutually aligned and engaged in intermolecular π···π or C−H···π[32] interactions. A closer examination of the pack structures in **1** and **2** shows that the driving forces for the formation of the bilayer arrangements are distinct: apparently, TCAS in **1** assembles into a bilayer arrangement mainly due to π···π interactions between the phenyl rings of the calixarenes, while the bilayer structure of CAS in **2** is constructed by C−H···π interactions between the methylene bridges and the aromatic rings of the calixarenes. As a result, the hydrophobic and hydrophilic layers are approximately in the region of 5.051 and 8.901 Å, with a repeat-distance sum of 13.952 Å, for the bilayer arrangement of TCAS in **1**, which is less than that of 15.275 Å for the CAS in **2**, which has a hydrophobic layer of 7.257 Å and a hydrophilic layer of 8.018 Å.

The guest molecule is influenced by the microenvironment of the calixarene host upon complexation. As can be seen from Figure 1 and Figure 4, the 2-DPD molecule in **1** adopts a *cis*-planar configuration, and the nitrogen atom of the pyridine ring embedded in the cavity of TCAS points towards the exterior of the cavity, while the 2-DPD molecule in **2** is found in a *trans* configuration, with the twist angle around the central carbon−carbon bond of 39.9°, and the nitrogen atom in the pyridine ring embedded in the cavity of CAS points towards the upper wall of the cavity. Both of them deviate from the stable *trans*-planar form in the crystalline state.[33] In crystal **1**, the pyridine ring in the 2-DPD molecule penetrating into the cavity of TCAS is not protonated, and the unprotonated nitrogen atom in the ring points away from the cavity, that is, the orientation of the pyridine ring is not arbitrary.[26d] On the other hand, the π···π interaction between the two 2-DPD molecules in a dimer (Figure 2; their centroid approach is 3.796 Å) is favorable for the two pyridine rings in each 2-DPD to assume a coplanar configuration. In addition, the strong N2−H2···O14 hydrogen-bonding interaction ($d_{H2\cdots O14}$ = 2.057 Å; $\Phi_{N2-H2\cdots O14}$ = 145.1°) together with the nonconventional C31−H31···O16 hydrogen bond($d_{H31\cdots O16}$ = 2.490 Å; $\Phi_{C31-H31\cdots O16}$ = 124.8°) further stabilize the *cis*-planar form of 2-DPD. It is interesting that the *cis*-planar configuration of 2-DPD is completely induced by noncovalent interactions, except the chelated-cis form in its metal chelate compounds.[34−36] In the crystal structure of **2** a nonconventional hydrogen bond between C35 in 2-DPD and O14 in the adjacent CAS makes the twisting angle of the two pyridine rings exceed the common range,[37] up to 39.9° in *trans* form.

As compared with the resulting bilayer supramolecular complexes **1** and **2** with 2-DPD, 4-DPD forms different host-guest complexes upon complexation with CAS and TCAS. Atwood et al.[29] have reported the crystalline complex of CAS with 4-DPD, in which CAS assumes a so-called 1,3-alternate conformation. Here we have prepared the crystalline complex of TCAS with 4-DPD (**3**) by hydrothermal synthesis, where the TCAS adopts a 1,2-alternate conformation (see a in Figure 6) and the 4-DPD moiety is stabilized by seven kinds of hydrogen bonding interactions between host and guest, as shown in Figure 6 (b). The conformation difference between TCAS and CAS may be attributed to the different bridge-linkages of TCAS and CAS, which provide the intrinsic features of their frameworks, such as flexibility. Furthermore, it is interesting to note that **3** and **4** present very similar physical properties, such as their yellow color, their high degree of stability, and their water insolubility, while both **1** and **2** are colorless crystals that are air-sensitive and water-soluble; this indicates that the different nitrogen position in DPD influences not only the conformational features of host molecules but also the physical properties of the complexes.

Complexation Thermodynamics

In order to investigate quantitatively the inclusion phenomena of the complexation of TCAS/CAS with the DPDs and illuminate further their binding ability and selectivity, an isothermal titration calorimetry (ITC) titration was performed at 25 °C in aqueous buffer solution to give the binding constants (K_S) and the thermodynamic parameters of 2-DPD and 4-DPD upon complexation with CAS and TCAS. The crystals were obtained in the acidic solution, so we also selected the corresponding condition for the isothermal calorimetric measurements. A phosphate buffer was chosen because it has no apparent influence on complexation, whereas other typical biological buffers tested previously interact with the calixarene sulfonates.[38]

A typical titration curve of TCAS with 2-DPD is shown in Figure 7; the thermodynamic parameters obtained are listed in Table 1. As expect, the obtained data are consistent with a 1:1 bonding model, although their binding ability

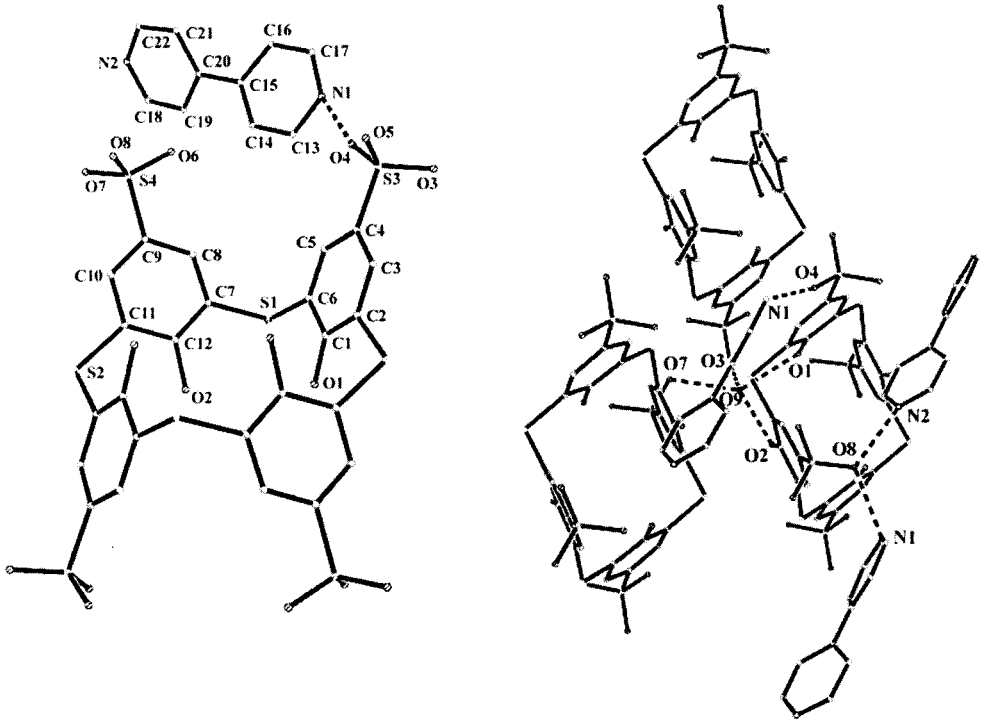

Figure 6. a) View of complex **3**, showing the so-called 1,2-alternate conformer; the other 4-DPDs, water molecules, and all the hydrogen atoms have been omitted for clarity; the broken line between O4 and N1 represents the host-guest hydrogen bonds; b) view showing the hydrogen-bonded network; hydrogen atoms have been omitted for clarity; H-bonds are drawn between donor and acceptor atoms (O1−O9: 2.873; N1−O4: 2.979; N1−O8: 3.096; O2−O9: 2.960; N2−O8: 2.862; O9−O3: 2.959; O9−O7: 2.955)

and thermodynamic parameters are entirely different from each other.

As shown in Table 1, the K_S values obtained for the complexation of TCAS/CAS with 2-DPD are larger than those with 4-DPD, i.e., 2.5 times for TCAS and 8.7 times for CAS. The crystal structures of complexes **1**−**4** are useful for our understanding these observations. Compared with 4-DPD in crystals **3** and **4**, 2-DPD in crystals **1** and **2** protrudes into the cavity of calixarenes, so the host-guest interaction between 2-DPD and TCAS/CAS is stronger than that of 4-DPD and therefore it forms more-stable inclusion complexes. Interestingly, although the replacement of bridging CH_2 groups in CAS by sulfides provides an enlargement of the cavity size for TCAS to accommodate more types of guest, the K_S values for the complexation of TCAS with DPD are smaller than those of CAS. Considering that electrostatic, hydrogen bonding, and π-stacking interactions exist in both cases, one reasonable explanation for the "abnormal" binding ability is that the van der Waal's interactions arising from the size/shape matching between CAS and DPD have a pronounced effect on the inclusion ability of CAS. The combination of these factors causes the exceptionally high binding constant for the complexation of CAS with 2-DPD.

The obtained thermodynamic data clearly indicate that the complexation of DPD with TCAS/CAS in aqueous phosphate buffer solution is exclusively driven by the large negative enthalpy changes ($-\Delta H^\circ$ = 18.0−36.7 kJ/mol), which are canceled in part by moderate entropy changes ($-T\Delta S^\circ$ = 2.5−13.8 kJ/mol), as shown in Table 1. In spite of the compensation between the negative ΔH° and $T\Delta S^\circ$, the complex stabilities (K_S) in aqueous phosphate buffer solution are completely different. As can be seen from Table 1, the complexation of TCAS/CAS with 2-DPD gives more-favorable enthalpy gains ($\Delta H^\circ_1 - \Delta H^\circ_3 = -9.5$ kJ·mol$^-$; $\Delta H^\circ_2 - \Delta H^\circ_4 = -12.2$ kJ·mol$^-$) than that of TCAS/CAS with 4-DPD. It is known that negative enthalpy contributions may arise mainly from the electrostatic, hydrogen bonding, π-stacking, and van der Waal's interactions during the course of the complexation of host with guest, and therefore the results could be attributed to the additional π-stacking and van der Waal's interactions between 2-DPD and TCAS/CAS that are observed in the resulting crystals. It is also noted that CAS gives a more-negative enthalpy change ($\Delta H^\circ_2 - \Delta H^\circ_1 = -9.2$ kJ·mol$^-$; $\Delta H^\circ_4 - \Delta H^\circ_3 = -6.5$ kJ·mol$^-$) upon complexation with DPDs than TCAS. In contrast, the complexation of TCAS/CAS with DPDs exhibits unfavorable entropy changes (−2.5 kJ/mol to −13.8 kJ/mol), and the global profiles of $T\Delta S^\circ$ is reversed as compared with the K_S values, that is to say, the smaller the entropy changes the higher the complex stability, and vice versa. It is reasonable to suppose that the negative entropy changes mainly result from the loss of conformational degrees of freedom for the hosts and struc-

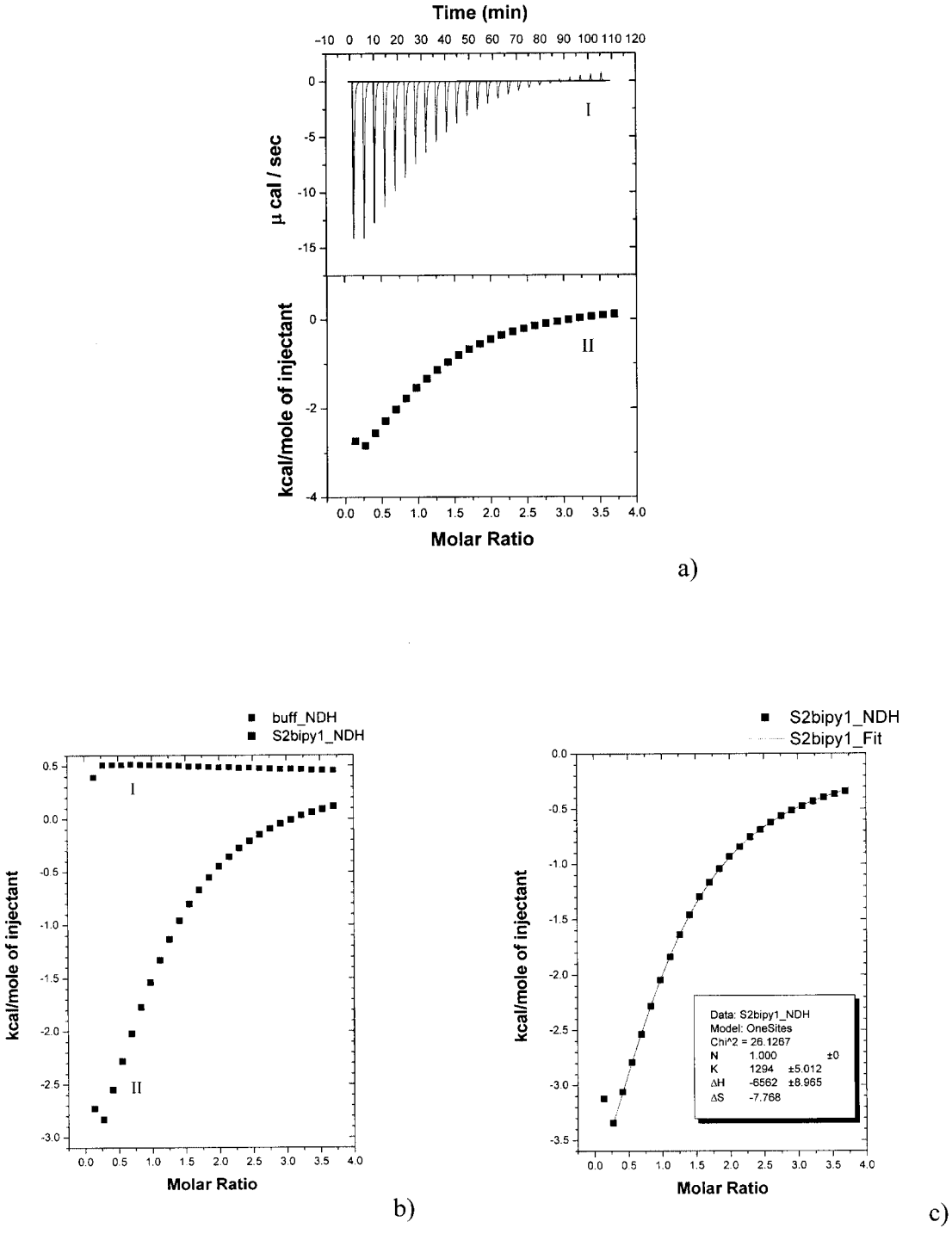

Figure 7. Calorimetric titration of 2-DPD with TCAS in aqueous solution at 25 °C; a) calorimetric titration of TCAS with 2-DPD in a phosphate buffer solution (pH 2.0) at T = 25 °C: (I) raw data for 25 sequential injections (10 μL per injection) of TCAS solution (20.12 mM) into 2-DPD solution (1.04 mM); (II) reaction heat obtained from the integration of the calorimetric traces; b) heat effects of the dilution (I) and the complexation reaction (II) of TCAS with 2-DPD for each injection during titration microcalorimetric experiments; c) "net" heat effects of complexation of TCAS with 2-DPD for each injection, obtained by subtracting the dilution heat from the reaction heat, which was fitted by computer simulation using the "one set of binding sites" model

tural freezing upon complexation, and the structurally slight difference between TCAS and CAS as well as between 2-DPD and 4-DPD would lead to the distinct $T\Delta S°$ values. Moreover, it is noted that the entropy loss upon complexation with the same guest molecules adds about 4.3 $kJ·mol^{-1}$ on going from TCAS to CAS, while upon complexation with the same host molecules it adds about 7.0 $kJ·mol^{-1}$ on going from 4-DPD to 2-DPD. The TCAS molecule possesses a larger cavity than CAS, so its loss of conformational degrees of freedom is certainly less, thus mak-

Table 1. Binding constants (K_S), standard enthalpy $\Delta H°$ (kJ·mol^{-1}), and entropy changes $T\Delta S°$ (kJ·mol^{-1}) for 1:1 inclusion complexation of TCAS and CAS with 2-DPD and 4-DPD at 25 °C in phosphate buffer solution (pH 2.0)

Reaction	[Guest] (mM)	[Host] (mM)	N[a]	K_S	$\Delta G°$ (kJ·mol^{-1})	$\Delta H°$ (kJ·mol^{-1})	$T\Delta S°$ (kJ·mol^{-1})
TCAS +2-DPD	1.04	20.12	2	1315 ± 20	−17.8 ± 0.0	−27.5 ± 0.1	−9.7 ± 0.1
CAS +2-DPD	0.52	10.24	2	10260 ± 190	−22.9 ± 0.0	−36.7 ± 0.2	−13.8 ± 0.3
TCAS +4-DPD	1.02	20.12	2	523 ± 7	−15.6 ± 0.1	−18.0 ± 0.1	−2.5 ± 0.2
CAS +4-DPD	0.51	10.24	2	1185 ± 2	−17.6 ± 0.1	−24.5 ± 0.1	−7.0 ± 0.1

[a] Number of microcalorimetric titration experiments performed.

ing the entropy losses upon complexation with DPDs smaller than with CAS. On the other hand, according to the crystal structures, the 2-DPD molecule possesses lower symmetry, which results in a relatively strong polarity as compared with that of 4-DPD,[30,39] and a stronger solvation degree, which making its desolvation difficult. In other words, the desolvation of 4-DPD is easier, which is well supported by the crystal structures of **3** and **4**: in **3** there are two water molecules in the unit cell, whereas in **4** no solvent water molecule is found.[29]

Conclusion

In conclusion, three inclusion complexes possessing the triclinic space group $P\bar{1}$ for **1**, the monoclinic space group $P2_1/n$ for **2**, and the triclinic space group $P\bar{1}$ for **3** were constructed by the complexation of CAS and TCAS with 2-DPD and 4-DPD. Crystallographic studies have shown that the calixarenes in **1** and **2** assemble themselves into bilayer aggregations, whereas **3** is a simple inclusion complex of TCAS with 4-DPD in which TCAS adopts a 1,2-alternate conformation. Further thermodynamic investigation has indicated that the enhanced complex stability is attributed to the enthalpy gains corresponding to the binding modes in the solid state. That is, deep inclusion of 2-DPD by CAS gives the largest binding constant and shows a highly molecular selectivity of up to nine times for the 2-DPD/4-DPD pairs. The obtained results reveal that the different positions of the nitrogen atoms in DPDs play a crucial role in controlling the molecular assemblies and thermodynamic properties of calixarenes, which is important for the design of supramolecular aggregations of calixarenes by finely manipulating the guest molecules.

Experimental Section

Materials and Instruments: 2,2′-Dipyridine and 4,4′-dipyridine are commercially available and were used without further purification. The *p*-sulfonatocalix[4]arene tetrasodium salt $Na^+_4CAS^-$ [7] and *p*-sulfonatothiacalix[4]arene tetrasodium salt $Na^+_4TCAS^-$ [16] were prepared according to the procedures reported before. According to the pK_a of the dipyridines,[40] the value of pH was maintained at less than 1 in the preparation of crystals of **1**−**4** to ensure that the dipyridines are diprotonated. Sodium dihydrogen phosphate was dissolved in distilled, deionized water to make a 0.1 mol·dm^{-3} phosphate solution, then was adjusted to pH 2.0 as a buffer solution by addition of H_3PO_4 for the isothermal calorimetric measurements.

Elemental analyses were performed on a Perkin−Elmer 2400C instrument.

The microcalorimetric titrations were performed on an isothermal titration microcalorimeter (VP-ITC), purchased from Microcal Co. (Northampton, MA) at atmospheric pressure and 25 °C in aqueous phosphate buffer solution (pH 2.0). pH 2.0 was chosen due to the restriction of the ITC equipment. In each run, a solution of host in a 0.250 mL syringe was sequentially injected with stirring at 300 rpm into a solution of guest in the sample cell (1.4227 mL volume). Each solution was degassed and thermostatted using a ThermoVac accessory before titration. A control experiment to determine the heat of dilution was carried out for each run by performing the same number of injections with the same concentration of host compound as used in the titration experiments into a pure buffer solution without the guest compound. The dilution enthalpies determined in control experiments were subtracted from the enthalpies measured in the titration experiments to obtain the net reaction heat.

The ORIGIN software (Microcal Inc.), which was used to simultaneously compute the equilibrium constant (K_S) and standard molar enthalpy of reaction ($\Delta H°$) from a single titration curve, gave a standard deviation based on the scatter of the data points in the titration curve. The net reaction heat in each run was calculated by the "one set of binding sites" model. Additionally, the first point was removed from the titration curve as the concentration of host in the cell far exceeded the concentration of the guest.

To check the accuracy of the observed thermodynamic quantities, two independent titration experiments were carried out; the average values obtained for the complex stability constant (K_S), standard free energy ($\Delta G°$), enthalpy ($\Delta H°$), and entropy changes ($T\Delta S°$) for 1:1 inclusion complexation of DPDs with TCAS or CAS are listed in Table 1.

Preparation of 1: Four equivalents of 2,2′-dipyridine was added to an aqueous solution of TCAS (0.05 mmol, 10 mL). Under stirring, 1 M HCl was dropped to adjust the pH to less than 1. After filtration, the filtrate was allowed to evaporate for about one week to yield 36 mg (56%) of **1**. The colorless crystalS formed were collected along with the mother liquor for the X-ray crystallographic analyses. $C_{49}H_{36}N_5O_{16}S_8·4.5H_2O$ (1288.4): calcd. C 45.68, H 3.52, N 5.44, S 19.91; found C 45.61, H 3.55, N 5.41, S 19.89.

Preparation of 2: CAS (0.05 mmol) was dissolved in 1 M HCl (10 mL), then 2 equiv. of 2,2′-dipyridine was added. After stirring for a few minutes, the solution was filtered and the filtrate was allowed to evaporate slowly for about two weeks to yield 32 mg (62%) of **2**. The colorless crystals formed were collected along with the mother liquor for the X-ray crystallographic analyses.

Table 2. Crystal structure data and details of structure refinements for **1**−**3**

	1	**2**	**3**
Formula	$C_{49}H_{45}N_5O_{20.50}S_8$	$C_{38}H_{47}N_2O_{23.50}S_4$	$C_{44}H_{36}N_4O_{18}S_8$
M_r (g mol^{-1})	1288.38	1036.02	1165.25
Crystal system	triclinic	monoclinic	triclinic
Space group	$P\bar{1}$	$P2_1/n$	$P\bar{1}$
Z	2	4	1
a (Å)	14.634(4)	12.133(4)	9.475(4)
b (Å)	14.812(4)	29.653(11)	10.311(5)
c (Å)	15.798(5)	12.323(5)	15.274(8)
α (°)	108.907(4)	90	73.379(6)
β (°)	101.396(4)	91.771(6)	84.377(6)
γ (°)	99.676(5)	90	79.072(5)
V (Å)	3074.7(15)	4431(3)	1402.3(11)
$\rho_{calcd.}$ (g cm^{-3})	1.392	1.553	1.380
$F(000)$	1332	2164	600
T (K)	293(2)	293(2)	293(2)
μ(Mo-K_α) (mm^{-1})	0.365	0.307	0.388
Crystal size (mm)	0.22 × 0.18 × 0.16	0.22 × 0.16 × 0.14	0.20 × 0.16 × 0.06
Range scanned θ (°)	1.74−25.00	1.37−25.01	2.09−25.01
Index range	$-15 \le h \le 17$	$-13 \le h \le 14$	$-11 \le h \le 11$
	$-15 \le k \le 17$	$-35 \le k \le 32$	$-12 \le k \le 11$
	$-18 \le l \le 17$	$-14 \le l \le 12$	$-18 \le l \le 9$
Reflections collected	15953	22572	5992
Unique reflections	10756	7812	4473
R_{int}	0.0349	0.0286	0.0799
R_1 [$I > 2\sigma(I)$]	0.0817	0.0620	0.1197
wR_2 (all data)	0.2956	0.1813	0.3581
(Δρ) max. (e·Å^{-3})	0.793	0.838	0.901
(Δρ) min. (e·Å^{-3})	−0.410	−0.565	−0.875

$C_{38}H_{32}N_2O_{16}S_4 \cdot 7.5H_2O$ (1036.0): calcd. C 44.05, H 4.57, N 2.70, S 12.38; found C 44.03, H 4.59, N 2.68, S 12.35.

Preparation of 3: TCAS (0.05 mmol) and 4,4′-dipyridine (4 equiv.) were suspended in 5 mL of water (pH < 1 adjusted by HCl) in a Teflon-lined stainless-steel bomb, which was then sealed, heated at 120 °C under hydrothermal conditions for 2 d, and then cooled gradually to room temperature at 2 °C per hour during about 3 d. The yellow, water-insoluble crystalline solid of **3** (45 mg, 78%) was collected and characterized by X-ray crystallographic analyses. $C_{44}H_{36}N_4O_{16}S_8 \cdot 2H_2O$ (1165.3): calcd. C 45.35, H 3.11, N 4.81, S 22.01; found C 45.38, H 3.15, N 4.78, S 21.98.

X-ray Crystal-Structure Determinations: The X-ray intensity data for **1**−**3** were collected on a standard Siemens SMART CCD Area Detector System equipped with a normal-focus molybdenum-target X-ray tube (λ = 0.71073 Å) operating at 2.0 kW (50 kV, 40 mA) and a graphite monochromator at T = 293(2) K. The structures were solved by direct methods and refined by full-matrix least-squares on F^2 (Siemens, SHELXTL-97). Summaries of crystal data and refinements are given in Table 2.

CCDC-246363 (for **2**), -246364 (for **1**), and -246365 (for **3**) contain the supplementary crystallographic data for this paper. These data can be obtained free of charge from The Cambridge Crystallographic Data Centre via www.ccdc.cam.ac.uk/data request/cif.

Acknowledgments

This work was supported by NNSFC (90306009, 20272028 and 20372038) and Tianjin Natural Science Foundation (No. 043604411), which are gratefully acknowledged.

[1] For books about calixarenes, see: [1a] C. D. Gutsche, *Calixarene Revisited*, in *Monographs in Supramolecular Chemistry* (Ed.: J. F. Stoddart), Royal Society of Chemistry, Cambridge, **1998**. [1b] L. Mandolini, R. Ungaro, *Calixarenes in Action*, Imperial College Press, London, **2000**. [1c] G. J. Lumetta, R. D. Rogers, A. S. Gopalan, *Calixarenes for Separations*, American Chemical Society, Washington D.C., **2000**.
[2] D. Diamond, K. Nolan, *Anal. Chem.* **2001**, *73*, 22A−29A.
[3] R. Ludwig, *Fresenius J. Anal. Chem.* **2000**, *367*, 103−128.
[4] A. Katz, P. D. Costa, A. C. P. Lam, J. M. Notestein, *Chem. Mater.* **2002**, *14*, 3364−3368.
[5] L. Baldini, C. Barcchini, R. Cacciapaglia, A. Casnati, L. Mandolini, R. Ungaro, *Chem. Eur. J.* **2000**, *6*, 1322−1330.
[6] A. Friggeri, F. C. J. M. van Veggel, D. N. Reinhoudt, *Chem. Eur. J.* **1999**, *5*, 3595−3602.
[7] G. Arena, A. Contino, G. G. Lombardo, D. Sciotto, *Thermochim. Acta* **1995**, *264*, 1−11.
[8] [8a] S. Shinkai, H. Koreishi, K. Ueda, T. Arimura, O. Manabe, *J. Am. Chem. Soc.* **1987**, *109*, 6371−6376. [8b] V. Ball, M. Winterhalter, F. Perret, G. Esposito, A. W. Coleman, *Chem. Commun.* **2001**, 2276−2277. [8c] A. Specht, P. Bernard, M. Goeldner, L. Peng, *Angew. Chem.* **2002**, *114*, 4902−4905; *Angew. Chem. Int. Ed.* **2002**, *41*, 4706−4708. [8d] S. Shinkai, K. Araki, T. Matsuda, N. Nishiyama, H. Ikeda, I. Takasu, M. Iwamato, *J. Am. Chem. Soc.* **1990**, *112*, 9053−9058. [8e] G. Arena, A. Casnati, A. Contino, G. G. Lombardo, S. Sciotto, R. Ungaro, *Chem. Eur. J.* **1999**, *5*, 738−744. [8f] S. Arimori, S. Shinkai, *J. Chem. Soc., Perkin Trans. 1* **1993**, 887−903. [8g] S. J. Dalgarno, M. J. Hardie, M. Makha, C. L. Raston, *Chem. Eur. J.* **2003**, *9*, 2834−2839. [8h] S. J. Dalgarno, C. L. Raston, *Dalton Trans.* **2003**, 287−290. [8i] J. L. Atwood, G. W. Orr, C. M. Means, F. Hamada, H. Zhang, S. G. Bott, K. D. Robinson, *Inorg. Chem.* **1992**, *31*, 603−606. [8j] J. L. Atwood, S. J. Dalgarno, M. J. Hardie, C. L. Raston, *New. J. Chem.* **2004**, *28*, 326−328.

[9] J. L. Atwood, L. J. Barbour, M. J. Hardie, C. L. Raston, *Coord. Chem. Rev.* **2001**, *222*, 3−32.
[10] A. W. Coleman, S. G. Bott, S. D. Morley, C. M. Means, K. D. Robinson, H. Zhang, J. L. Atwood, *Angew. Chem.* **1988**, *110*, 1412−1413; *Angew. Chem. Int. Ed. Engl.* **1988**, *27*, 1361−1362.
[11] H. R. Webb, M. J. Hardie, C. L. Raston, *Chem. Eur. J.* **2001**, *7*, 3616−3620.
[12] G. W. Orr, L. J. Barbour, J. L. Atwood, *Science* **1999**, *285*, 1049−1052.
[13] P. J. Nichols, C. L. Raston, J. W. Steed, *Chem. Commun.* **2001**, *12*, 1062−1063.
[14] [14a] H. Kumagai, M. Hasegawa, S. Miyanari, Y. Sugawa, Y. Sato, T. Hori, S. Ueda, H. Kamiyama, S. Miyano, *Tetrahedron Lett.* **1997**, *38*, 3971−3972. [14b] N. Iki, C. Kabuto, T. Fukushima, H. Kumagai, H. Takeya, S. Miyanari, T. Miyashi, S. Miyano, *Tetrahedron* **2000**, *56*, 1437−1443.
[15] [15a] N. Iki, S. Miyano, *J. Inclusion Phenom. Macrocyclic Chem.* **2001**, *41*, 99−105. [15b] P. Lhotak, *Eur. J. Org. Chem.* **2004**, 1675−1692.
[16] N. Iki, T. Fujimoto, S. Miyano, *Chem. Lett.* **1998**, 625−626.
[17] N. Iki, T. Fujimoto, T. Shindo, K. Koyama, S. Miyano, *Chem. Lett.* **1999**, 777−778.
[18] N. Iki, T. Suzuki, K. Koyama, C. Kabuto, S. Miyano, *Org. Lett.* **2002**, *4*, 509−512.
[19] N. Kon, N. Iki, S. Miyano, *Org. Biomol. Chem.* **2003**, *1*, 751−755.
[20] N. Iki, T. Horiuchi, H. Oka, K. Koyama, N. Morohashi, C. Kabuto, S. Miyano, *J. Chem. Soc., Perkin Trans. 2* **2001**, 2219−2225.
[21] T. Horiuchi, N. Iki, H. Oka, S. Miyano, *Bull. Chem. Soc., Jpn.* **2002**, *75*, 2615−2619.
[22] H. Matsumiya, T. Ishida, N. Iki, S. Miyano, *Anal. Chim. Acta* **2003**, *478*, 163−170.
[23] Y. Liu, H. Wang, L.-H. Wang, H.-Y. Zhang, *Thermochim. Acta* **2004**, *414*, 65−70.
[24] M. Hiroaki, M. Hideharu, T. Yukiko, N. Iki, S. Miyano, *Bull. Chem. Soc. Jpn.* **2003**, *76*, 133−136.
[25] S. K. Mate, K. Szabo, I. Bitter, G. Nagy, L. Kollar, *Tetrahedron Lett.* **2004**, *45*, 1387−1390.
[26] [26a] D. Yuan, W.-X. Zhu, S.-L. Ma, X. Yan, *J. Mol. Struct.* **2002**, *616*, 241−246. [26b] Q.-L. Guo, W.-X. Zhu, S.-J. Dong, S.-L. Ma, X. Yan, *J. Mol. Struct.* **2003**, *650*, 159−164. [26c] Q.-L. Guo, W.-X. Zhu, S.-L. Ma, D.-Q. Yuan, S.-J. Dong, M.-Q. Xu, *J. Mol. Struct.* **2004**, *690*, 63−68. [26d] Q.-L. Guo, W.-X. Zhu, S. Gao, S.-L. Ma, S.-J. Dong, M.-Q. Xu, *Inorg. Chem. Commun.* **2004**, *7*, 467−470.
[27] Y. Liu, D.-S. Guo, H.-Y. Zhang, *J. Mol. Struct.*, in press.
[28] P. C. Leverd, P. Berthault, M. Lance, M. Nierlich, *Eur. J. Org. Chem.* **2000**, 133−139.
[29] L. J. Barbour, J. L. Atwood, *Chem. Commun.* **2001**, 2020−2021.
[30] Y. Liu, Y.-L. Zhao, H.-Y. Zhang, E.-C. Yang, X.-D. Guan, *J. Org. Chem.* **2004**, *69*, 3383−3390.
[31] J. L. Atwood, G. W. Orr, F. Hamada, R. L. Vincent, S. G. Bott, K. D. Robinson, *J. Am. Chem. Soc.* **1991**, *113*, 2760−2761.
[32] S. J. Dalgarno, C. L. Raston, *Chem. Commun.* **2002**, 2216−2217.
[33] L. L. Merritt Jr., E. D. Schroeder, *Acta Crystallogr.* **1956**, *9*, 801−804.
[34] K. Nakamoto, *J. Phys. Chem.* **1960**, *64*, 1420−1425.
[35] G. H. Stewart, H. Eyring, *J. Chem. Educ.* **1958**, *35*, 550−557.
[36] H. J. Dothie, F. J. Llewellyn, W. Wardlaw, A. J. E. Welch, *J. Chem. Soc.* **1939**, 426−428.
[37] P. E. Fielding, R. J. W. LeFevre, *J. Chem. Soc.* **1951**, 1811−1814.
[38] N. Douteau-Guével, F. Perret, A. W. Coleman, J. P. Morel, N. Morel-Desrosiers, *J. Chem. Soc., Perkin Trans. 2* **2002**, 524−532.
[39] U. S. Schubert, C. Eschbaumer, *Angew. Chem. Int. Ed.* **2002**, *41*, 2892−2926.
[40] pK_{a1} = −0.52, pK_{a2} = 4.35 for 2,2′-dipyridine; pK_{a1} = 3.17, pK_{a2} = 4.82 for 4,4′-dipyridine (from *Handbook of Physical Chemistry*).

Received September 1, 2004

